Palaeogeography, Palaeoclimatology, Palaeoecology 538 (2020) 109462

Contents lists available at ScienceDirect

Palaeogeography, Palaeoclimatology, Palaeoecology

journal homepage: www.elsevier.com/locate/palaeo

Pastoralism increased vulnerability of a subalpine catchment to flood hazard through changing soil properties

Manon Bajard[a,b,*], Jérôme Poulenard[b], Pierre Sabatier[b], Yann Bertrand[b], Christian Crouzet[c], Gentile Francesco Ficetola[d,e], Claire Blanchet[b], Erwan Messager[b], Charline Giguet-Covex[b], Ludovic Gielly[d], Delphine Rioux[d], Wentao Chen[d], Emmanuel Malet[b], Anne-Lise Develle[b], Fabien Arnaud[b]

[a] Centre for Earth Evolution and Dynamics, University of Oslo, PO Box 1028, Blindern, 0315 Oslo, Norway
[b] Univ. Grenoble Alpes, Univ. Savoie Mont Blanc, CNRS, EDYTEM, 73000 Chambéry, France
[c] ISTerre, Univ. Grenoble Alpes, Univ. Savoie Mont Blanc, CNRS, 73000 Chambéry, France
[d] LECA, CNRS UMR 5553, Université Grenoble Alpes, 38041 Grenoble, France
[e] Department of Environmental Science and Policy, Università degli Studi di Milano, Milan 20133, Italy

ARTICLE INFO

Keywords:
Lake sediments
Pedogenesis
Weathering
Pastoralism
Climate
Erodibility

ABSTRACT

Soil erosion is strongly linked to both precipitation patterns and land-use. We examine the effects of erosion and its drivers (*i.e.* human or/and climate) on soil evolution from the study of lacustrine archives in the northern French Alps. Multi-proxy analyses of the Lake Gers sediment sequence combined with the study of soils and rocks of its catchment allowed to reconstruct its evolution over the past 4.6 kyr. This included ^{14}C dating, short-lived radionuclides, geochemistry, loss on ignition, grain-size analyses, as well as plant and mammal DNA analyses. A total of 127 instantaneous deposits were identified among the continuous sedimentation in the lake and 93 were interpreted as flood deposits. Erosion was quantified for the whole catchment considering both the continuous sedimentation and the flood deposit thicknesses.

The catchment is mainly formed by andesitic sandstones over which Andosols and Podzols can develop. However, low weathered materials from colluviation constitute the main input to the lake.

Four main phases of changes in soil weathering were recorded by increases in K_2O/TiO_2 ratios, associated with an increase in both erosion and flood-frequency. Two phases were associated with climate cooling in the Western Alps, from 2.65 to 2.5 and from 1.45 to 1.3 cal kyr BP. The two others (1.9–1.75 and 0.9–0.4 cal kyr BP) were triggered with deforestation, with cow grazing during the Roman period, and with grazing of cows, sheep and goats during the Medieval period, amplified by the onset of the Little Ice Age. The increase in erosion and flood frequency after 950 cal yr BP indicates substantial damages to soils of the catchment including increase of their erodibility over the last millennia.

1. Introduction

Erosion is a natural process, commonly occurring in mountain areas due to steep slopes and high precipitation (Verheijen et al., 2009). Torrential flooding transport mechanisms are often studied for flood hazards and for climatic impacts, which are exacerbated by snow melting in spring or intense stormy rainfall in summer and fall (Noren et al., 2002; Wilhelm et al., 2012; Sabatier et al., 2017; Wilhelm et al., 2018). Few studies focus on the long term effects of flood-triggered erosion on soil evolution despite the fact that landscape, that are based on the soil cover, may be threatened by flood events. Soils provide numerous ecosystem services, including supporting, provisioning and regulating services, as food production, regulation of climate disruption by carbon storage and flood mitigation (Daily et al., 1997; MEA, 2005; Adhikari and Hartemink, 2016). The loss of soil thickness is frequently associated to loss of soil properties like structure or organic matter content (Stacy et al., 2015; Wang et al., 2017). This can decrease the potential of water infiltration and storage and favor surface runoff, through Horton overland flow, thus further increasing erosion (Bailey et al., 1934). The loss of soils in upstream mountain catchments induces more direct and rapid concentration of waters and thus can have strong effect on valley flooding, where infrastructures and housing are

* Corresponding author at: Centre for Earth Evolution and Dynamics, University of Oslo, PO Box 1028, Blindern, 0315 Oslo, Norway.
E-mail address: manon@geo.uio.no (M. Bajard).

https://doi.org/10.1016/j.palaeo.2019.109462
Received 10 July 2019; Received in revised form 25 October 2019; Accepted 12 November 2019
Available online 18 November 2019

concentrated. This displacement of soil and sediments can also result in deep hydrological changes in the catchment. The consequences of floods are thus doubled, with the potential mobilization of large amount of soil associated with ecological and economical losses, as well as the transfer of large amount of water downstream, threatening societies. If flooding are necessary triggered by precipitation, their effects on erosion can be increased according to the conditions of the catchment, especially in response to human-induced modifications (Cosandey et al., 2005; Giguet-Covex et al., 2011; Brisset et al., 2017). Therefore, it is necessary to dissociate what is climate or human induced in flood related erosion, and take interest in land use modifications.

Both the number and intensity of extreme precipitations and thus, flood events, are expected to increase with the climate warming in several places in the world and especially in mountainous areas (Giorgi et al., 2016). Consequences of the global warming will also affect lands and agriculture systems as highlighted recently by the IPCC Special Report on Climate Change and Land (IPCC, 2019). In this context, it becomes essential to understand how soils can react and be disrupted by flood and land use change to adapt environmental practices and management in the upstream, thereby ensuring safe living accommodation and sustainability of the agro-pastoral practices. Upstream areas are usually neglected in risk prevention plans or adaptation to climate change because they are considered as natural areas and located usually far from human properties values.

Paleo-environmental reconstructions from lake sediments offer the opportunities to study at the same time soil evolution, flood-frequency and effect of human activities on long time-scale (Giguet-Covex et al., 2011, 2014; Arnaud et al., 2016; Brisset et al., 2017). Lake sediment archives are useful to reconstruct past flood events, especially in mountainous areas (Noren et al., 2002; Moreno et al., 2008; Wilhelm et al., 2012; Wirth et al., 2013; Sabatier et al., 2017; Fouinat et al., 2017a; Wilhelm et al., 2019). They also can be used to reconstruct past land use and agricultural activities from pollen and non-pollen palynomorph analyses (Doyen and Etienne, 2017) and from plant and mammal DNA (*e.g.*, animal husbandry) (Giguet-Covex et al., 2014; Parducci et al., 2017; Sabatier et al., 2017; Bajard et al., 2017b). Soil evolution is reconstructed from the comparison between the lake archives and the current soils (Ewing and Nater, 2002; Mourier et al., 2008; Giguet-Covex et al., 2011; Bajard et al., 2017a, 2017b).

Here we present a study based on a lake sediment sequence of the Northern French Alps with the objectives to i) identify flood deposits and establish a flood chronicle, ii) understand the soil evolution, applying a source-to-sink approach (*i.e.*, combining catchment samples and lake sediment analyses) and to iii) link soil evolution and flood-frequency with external anthropic and/or climate forcing.

2. Materials and methods

2.1. Study site

Lake Gers (46°1′36″N, 6°43′45″E, 1540 m a.s.l.) is located in the Northern French Alps (Fig. 1a) on the municipality of Samoëns in the Giffre river Valley. The area of the lake is 0.05 km^2 and its maximum depth is 5.6 m (Sesiano, 1993). The lake level decreases of 2 m between spring and summer because of loss of water under the lake (Fig. 1b). The lake is fed by a temporary stream that mainly drains the west side of the catchment. The catchment covers an area of 5 km^2 and rises up to 2385 m a.s.l. (Fig. 1c). The lake is of glacial origin and is part of the Giffre river catchment.

According to the weather observation network of the alpine massif (ROMMA), the mean temperatures at Arâches-La Frasse, located at 8 km west from Lake Gers at 1120 m and corrected of an altitudinal gradient of −0.5 °C/100 m for Lake Gers altitude, range from −1.2 °C in winter to 13.0 °C in summer (these values represent averages for 2011–2017). Precipitations are approximately 1500 mm per year. Snow covers the area from December to April, and the lake is ice-covered during winter. Avalanches fall out every winter and early spring, especially from the west side of the lake, and can reach the lake.

The bedrock of the catchment is dominated by Taveyannaz sandstones of Eocene-Oligocene ages (Fig. 1c), which are composed by approximately 80% of volcanic materials associated with a carbonated matrix (Martini, 1966). Within the sandstones, carbonated marly levels can outcrop in some points of the catchment (*e.g.*, GERS3, GERS4).

Picea abies is the main tree species covering the east side of the lake (Fig. 1c and d). Pastured grasslands cover the south edge of the lake and the upstream of the catchment with punctual areas colonized by *Ericaceae* (*Vaccinium myrtillus*, *Vacciniumuliginosum*, *Rhododendron ferrugineum*). Alder (*Alnus viridis*) concentrates in the middle of the catchment and in avalanche areas (Fig. 1c and d).

2.2. Soil sampling

Eleven soil profiles (GERS1 to 11) were realized in Lake Gers catchment to characterize the major soil types. Soil profiles were described with color, texture, structure and HCl effervescence test. The FAO (Food and Agriculture Organization) soil classification (WRB - FAO, 2014) and the Guidelines for soil description (FAO, 2006) were used for horizon and soil denominations. At least one sample was collected per horizons and sieved to 2 mm for further laboratory analyses. When it was possible, samples for density estimation were taken with a cylinder. Parent materials from these soils were also collected for geochemical comparison. Soil pH (n = 3) were measured for each horizon with a 1:5 soil-water ratio.

2.3. Lake sediment cores

Two coring campaigns were undertaken to retrieve sediments from the deepest part of Lake Gers in winter 2015 and winter 2016. Short gravity cores were taken in 2015 from the ice-covered surface to provide a well-preserved water-sediment interface. Two longer overlapping sections (GER16-I and GER16-II) that are approximately 6 m each in length were retrieved in 2016 (Fig. 1b) using an Uwitec piston coring device. The cores were split into two halves. Each half was described in detail, and pictures were taken with a 20-pixel·mm^{-1} resolution. The lithological description of the cores allowed the identification of different sedimentary units. A composite profile of 5.8 m (GER16) was built with lithological correlation from a short gravity core (GER15_P3) obtained in 2015 (IGSN code: IEFRA05HV; *IGSN codes refer to an open international database*, *www.geosamples.org*) and the two sedimentary sections obtained during the 2016 coring. One half of the core was used for non-destructive analysis (*i.e.*, XRF core scanner) and the other half for sampling and performed destructive analysis.

2.4. Analysis performed on both catchment and lake sediment samples

2.4.1. Loss on ignition

Loss on ignition (LOI) analysis was performed on both the soil samples and sediments, every 2 cm all along the sediment sequence to estimate the organic matter (OM) and carbonate contents following the procedure described in Heiri et al. (2001). A measure of density was also realized every 2 cm on the sediment core, by sampling and weighting known volume of sediment before the LOI measures.

2.4.2. P-XRF mineral geochemistry

A portable ED-XRF spectrometer (S1 TITAN Bruker) was used on soils, rocks and lake sediments to have a quantitative and comparative measurement of major elements, which were expressed as relative percentages of oxides. Analysis of gently crushed soil and sediment and crushed rocks samples was performed through a 4-μm-thick Ultralene film in a 32-mm-diameter plastic cup. The samples were triplicated and analyzed over 60 s using the GeoChem Standard instrument's internal

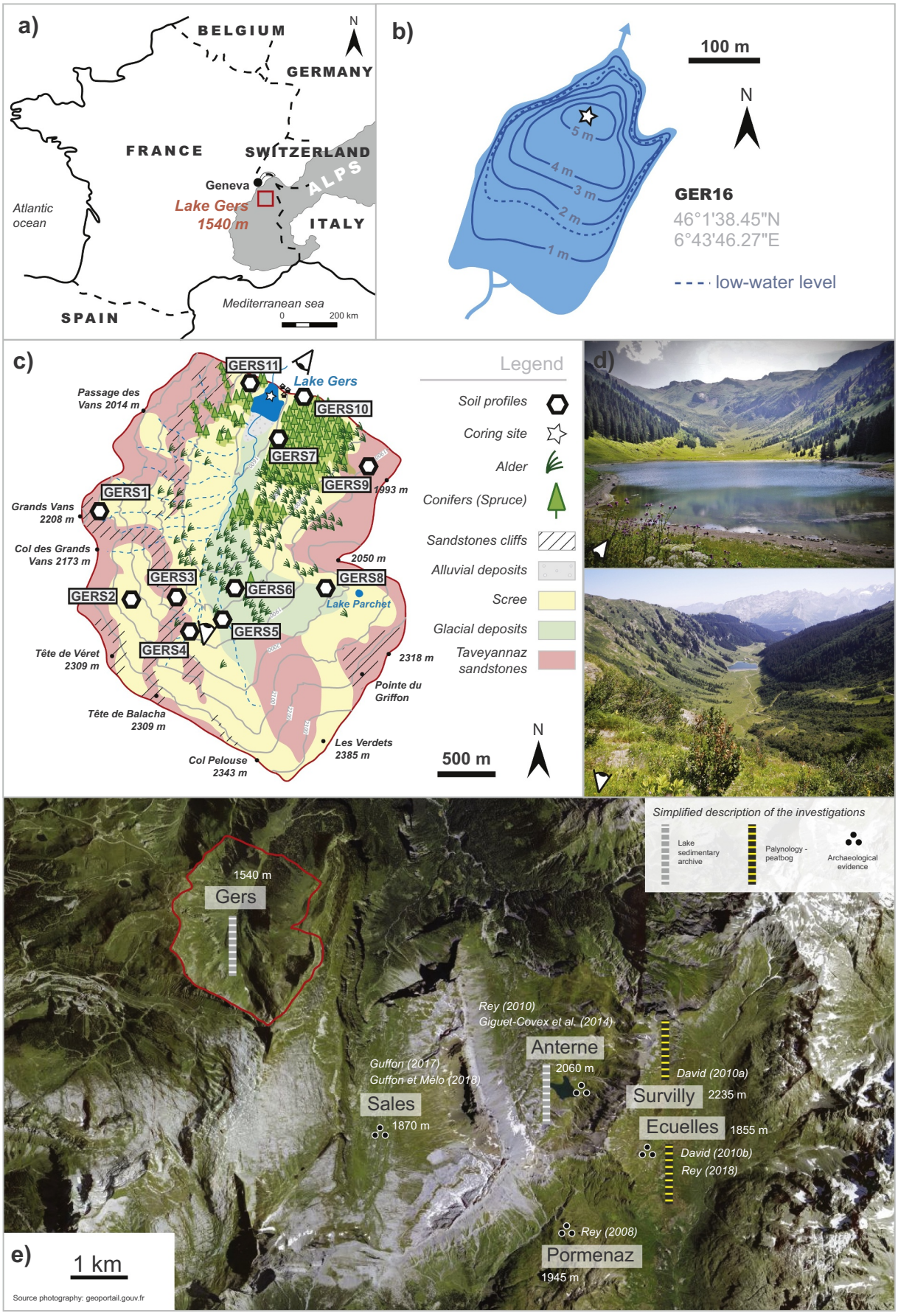

(caption on next page)

Fig. 1. Location of Lake Gers in the Western Alps (a) with the bathymetry of the lake (b) adapted from Sesiano (1993), the simplified geological map of the catchment with the location of the soil profiles (c), the views from the north and south sides of the lake catchment (d) and locations of the nearest sites referenced in the discussion (e).

calibration mode (Shand and Wendler, 2014). The standard deviations of the replicates were lower than the instrument errors, which were thus conserved as measurement uncertainties. The total contents of Si, Fe Al and Mn were estimated from SiO_2, Fe_2O_3, Al_2O_3 and MnO contents, respectively. Principal component analysis (PCA) was performed on the P-XRF geochemical data from rock and soil samples in order to identify similar rock samples and associated similar soil processes. Analyses were performed using R 2.13.1 (R Development Core Team, 2011).

2.5. Analysis performed only on lake sediments

2.5.1. XRF Core Scanner

The relative contents of chemical elements were analyzed by X-ray fluorescence (XRF) at high resolution (2 mm sampling step) on the surface of the sediment core with an Avaatech core scanner (EDYTEM Laboratory, CNRS-Université Savoie Mont-Blanc). The core surface was first covered with a 4-µm-thick Ultralene film to avoid contamination and desiccation of the sediment. The element intensities were expressed in counts per second (cps). Geochemical data were obtained with different settings according to the elements analyzed. These settings were adjusted to 10 kV and 1.5 mA for 10 s to detect Si, Ca, Al, Fe, Ti, K, Mn, and S. For heavier elements (*i.e.* Sr, Rb, Zr, Br, and Pb), measurements were performed at 30 kV and 1.0 mA for 40 s.

2.5.2. Sedimentary environmental DNA (sedDNA)

To reconstruct the past vegetation dynamic and the nature of herds (*i.e.*, cows, sheep and goats) by DNA analysis, we sampled 35 slices of 1 to 2-cm thickness covering the whole sediment core, following the strict laboratory precautions described in Giguet-Covex et al. (2014). Extracellular DNA was extracted from the sediment, amplified within 8 PCR replicates and sequenced as described in Supplementary materials. The sequence analyses were performed using the Obitools software (https://git.metabarcoding.org/obitools/obitools/wikis/home) (Boyer et al., 2016). For mammals, we only kept sequences with a match > 97% with the sequences in the reference database and removed all the sequences assigned to hominideae. Results are given in number of positive PCR replicates. For plants, we only considered sequences with a match > 95% with the sequences in the reference database. Then, several filtering steps were applied to remove the potential contaminants (see Supplementary materials for more details). The contribution of each taxon and then of vegetation types were obtained by doing the sum of the number of reads from each replicate and for each taxon. Then, we log-transformed these numbers (log (N reads + 1)) to correct from the exponential increase of DNA sequences during the PCR amplification. We calculated the taxon contribution from these log-transformed read numbers.

2.5.3. Chronology

The chronology of the sediment sequence is based on ten ^{14}C measurements performed on terrestrial plant macroremains, as well as on short-lived radionuclide measurements (^{210}Pb and ^{137}Cs). AMS (accelerator mass spectrometer) radiocarbon dates were performed by the Poznan Radiocarbon Laboratory and the Laboratoire de Mesure 14C (LMC14) ARTEMIS at the CEA (Atomic Energy Commission) Institute of Saclay. The ^{14}C ages were calibrated using the IntCal13 calibration curve (Reimer et al., 2013). Short-lived radionuclides were used to date the most recent sediments. They were measured on the upper 24 cm of GER15_P3 gravity core at the Modane Underground Laboratory (LSM). Measurements were performed by gamma spectrometry, using high-efficiency, very low-background, well-type Ge detectors (Reyss et al., 1995). ^{137}Cs was first introduced in the environment at the end of the 1950s as by-product of atmospheric nuclear weapons tests (maximum peak at 1963 CE in the Northern Hemisphere). The Chernobyl accident in 1986 also dispersed ^{137}Cs into the Northern Hemisphere (Appleby et al., 1991). ^{210}Pb excess activities ($^{210}Pb_{ex}$) are calculated in the sediment as the difference between total ^{210}Pb (mixing of erosion and atmospheric deposits) and ^{226}Ra activities at each levels (Goldberg, 1963). Then, we used the Constant Flux/Constant Sedimentation (CFCS) model and the decay of $^{210}Pb_{ex}$ to calculate the mean sedimentation rates. The uncertainty of sedimentation rates obtained with this method is derived from the standard error of the linear regression of the CFCS model. The age–depth model for the entire sequence associating short-lived radionuclides and ^{14}C was then generated using R software and the R code package 'Clam' version 2.2 (Blaauw, 2010).

2.5.4. Estimating erosion

The erosion was estimated from the lake filling considering the volume of each layer of sediment in the lake, their dry densities, their corresponding sedimentation rate and the surface of the catchment (5 km^2), following the method described in Bajard et al., 2017a. We estimated the volume from the surface corresponding to the current higher lake level of the lake (0.05 km^2) and the depths in the core, assuming the sediment is equally distributed on the entire surface area of the lake (Enters et al., 2008). The approximations made on the calculation of the volume are expected to overestimate the accumulated mass of sediment, because of the higher accumulation in the deepest part of the lake, where the core was taken. However, the progradation of the delta should cause the opposite effect and reduce the overestimation. The mass of sediment was then calculated for each sampled depth, using the dry density. Only the non-carbonate terrigenous mass of the sediments was considered, using the Non-Carbonate Ignition Residue (NCIR) of the LOI. The terrigenous masses of each depth were then integrated according to the time, using the age-depth model, and divided by the surface of the catchment to estimate the erosion rate per unit area.

3. Results

3.1. Identification and formation of soils of the catchment

Three main types of pedogenetic processes, *i.e.*, andosolization, podzolization and colluviation were identified in the catchment of Lake Gers (Fig. 2 and Table 1). A complete description of the soils is presented in Supplement material.

Cambisols (GERS1, GERS2, GERS11 and GERS5) present mainly a succession of different brown horizons. They are characterized by low pH increasing with depth and decreasing OM content (Fig. 2 and Table 1). Andosols as GERS8 present a darker color due to high OM content throughout the profile and their pH is low (Fig. 2). They develop on Taveyannaz sandstones which are made of 80% of volcanic materials (Martini, 1966) that make possible the andosolization in this area. They also displays the lowest K_2O/TiO_2 ratio (Table 1). Podzols as GERS6, GERS7, GERS9 and GERS10 are characterized by low pH and decreasing OM content in the profile. Colluviation is characterized by lots of coarse elements, higher pH and low OM contents (GERS3, GERS4 and GERS11 in Fig. 2). These soils also display the highest K_2O/TiO_2 ratios (Table 1).

The PCA performed on the geochemistry of both the rocks and soils samples allowed to better understand the soil formation and identify different geochemical sediment sources (Fig. 3).

Dimensions 1 and 2 (denoted as *Dim 1* and *Dim 2*) of the PCA from

ANDOSOLIZATION

Andic Cambisols (GERS1 and GERS2)

GERS2

46° 0'43,60"N
6°43'1,50"E
2085 m
Vaccinium

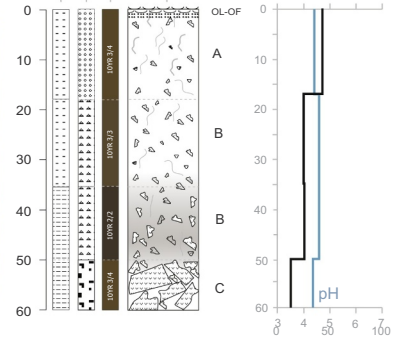

Andosols

GERS8

46°00'46,1" N
6°44'7,7" E
2016 m
Vaccinium

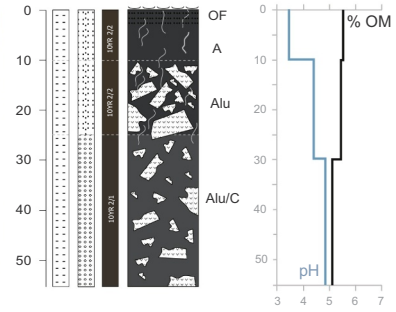

PODZOLIZATION

Cambisols (GERS5) to Entic Podzols (GERS6, GERS7, GERS10)

GERS6

46° 0'45,00"N
6°43'35,40"E
1880 m
Alder

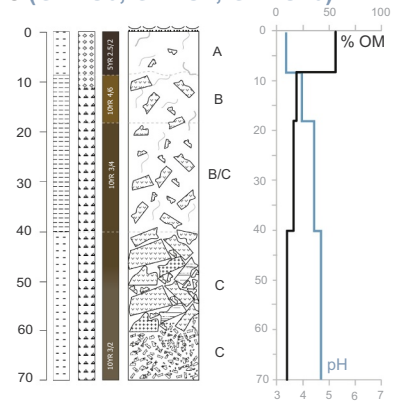

Podzols

GERS9

46° 1'16.20"N
6°44'23.20"E
1990 m
Matgrass

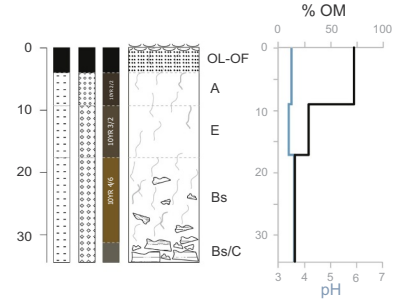

COLLUVIATION

Colluvic Regosols (GERS3, GERS4) and Colluvic Cambisols (GERS11)

GERS11

46° 1'40,60"N
6°44'39,80"E
1573 m

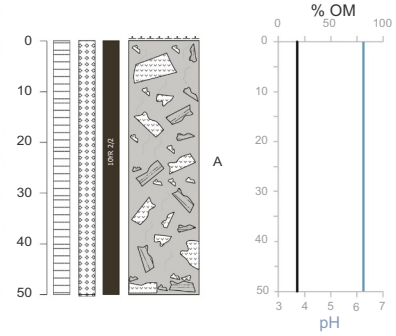

Legend

Texture
- Silty Loam
- Clay Loam
- Silty Clay

Structure
- Lumpy
- Subangular blocky
- Blocky
- Smeary

Artefacts

Coarse elements
- Taveyannaz sandstone with decarbonatation halo
- Marly carbonated facies whithin Taveyannaz sandstone
- **Roots** : fine, medium, coarse

(caption on next page)

Fig. 2. Pedologic description of the soil profiles (texture, structure, color) with organic matter content (OM), pH measures with horizons (WRB - FAO, 2014).

the geochemical data of the parent materials represent 75.6% of the total variability (Fig. 3a). Three end members were identified on the correlation circle. The first one includes TiO_2 as well as Fe_2O_3 and SiO_2 and is positively correlated with the first dimension of the PCA. It concerns rocks from GERS1, GERS2 and GERS8 (Fig. 3a). Al_2O_3 forms a single end member, positively correlated with the second component of the PCA. This second end member contains the parent materials of GERS5, GERS6 and GERS9. The third one is negatively correlated with both components and gives positive loading between K_2O and CaO. This third end member contains the rocks sample of GERS3 and GERS4. Parent materials of GERS11 are located between these three end-members (Fig. 3a).

The PCA performed with soil samples includes the same geochemical elements than the rock sample PCA (SiO_2, Al_2O_3, TiO_2, Fe_2O_3, CaO) and the OM content (Fig. 3b). Dimensions 1 and 2 represent 78% of the total variability of this dataset. Dimension 1 gives positive loading to Fe_2O_3 and negative loadings to K_2O. TiO_2 and the OM content are correlated to both dimensions. Dimension 2 (Dim 2) gives negative loading to Al_2O_3 and CaO but CaO is poorly representative in the soil dataset (Fig. 3b). SiO_2 is positively correlated to Dim 2 and negatively to Dim 1. Surface horizons are associated with OM direction and conversely, the deepest horizons are anticorrelated to OM. Samples from GERS9, GERS6 and GERS5 are mainly associated with Dim 2 and form a "Podzolic" endmember. GERS4 and GERS11 are anticorrelated to Dim 1 and closely associated to K_2O (Fig. 3b). They form an end-member of low weathered soils, with the deepest horizons of other soils. GERS1, GERS2 and GERS8 appear to be mainly associated to Fe_2O_3 and Al_2O_3 and form an "Andic" endmember. GERS7 is in the center of the PCA.

3.2. Core description and lithology

The continuous sedimentation of the 5.8 m of the sequence consists mainly of dark medium silts, with a higher variability between 3 and 1.25 m. The organic matter content is 11% in average and the carbonate content is 3% in average.

The sedimentary sequence is interrupted by 127 individual layers that are interpreted as short-term depositional events according to Sturm and Matter (1978) and Arnaud et al. (2002). 93 of these deposits are darker graded beds with a coarse and no erosive base and present thicknesses ranging from the millimeter to the dozens of centimeters. The thickest deposits occur at 5.20 m (12 cm), 3.90 m (9.5 cm), 3.02 m, (13.5 cm), 1.73 m (6.5 cm) and 1.31 m (11 cm). Between 1.80 and 2.00 m, deposits are thinner and more numerous (approximately 30 between 2 and 8 mm of thickness).

The 34 other deposits are very fine sand layers from < 1 mm to 5 mm, located only in the bottom part of the core, between 4.8 and 5.8 m.

A more complete description of the sediment analyses according to depth is presented in the Supplementary materials.

3.3. Age-depth model and instantaneous deposits

3.3.1. Short-lived radionuclides

The measurement of short-lived radionuclides allowed the dating of the uppermost 16 cm of the core. A logarithmic plot of $^{210}Pb_{ex}$ activity (Fig. 4a) shows a downward decrease from the surface. The three deepest points measured were rejected because of their distance from

Table 1
Soil horizon analyses of the catchment of Lake Gers.

	Sample	Top depth (cm)	Bottom depth (cm)	Horizon	pH_{water}	Bulk density	OM % (LOI 550 °C)	Al_2O_3%	SiO_2%	K_2O %	CaO %	TiO_2%	MnO %	Fe_2O_3%	Zr %	Total %	K_2O/TiO_2
	GERS1																
GERS 1–1	1–1	0	17	A	4.0	0.5	57.0	7.62	23.85	1.07	0.62	1.03	0.08	7.75	0.03	99.1	1.0
GERS 1–2	1–2	17	45	B	4.2	–	26.2	18.31	38.39	1.79	1.18	1.49	0.15	11.29	0.04	98.9	1.2
GERS 1–3	1–3	45	65+	C	5.0	–	7.8	19.65	57.04	2.28	2.31	1.12	0.10	9.10	0.04	99.5	2.0
	GERS2																
GERS 2–1	2–1	0	17	A	4.4	–	43.3	10.71	32.34	1.31	0.80	1.10	0.17	9.44	0.04	99.2	1.2
GERS 2–2	2–2	17	35	B	4.6	–	25.1	16.51	41.95	1.65	1.20	1.36	0.22	11.15	0.04	99.2	1.2
GERS 2–3	2–3	35	50	B	4.6	–	25.8	20.44	38.27	1.71	1.86	1.18	0.13	9.77	0.05	99.2	1.5
GERS 2–4	2–4	50	60+	C	4.3	–	13.0	22.03	48.87	2.26	3.00	1.08	0.10	9.19	0.04	99.6	2.1
	GERS4					–											
GERS 4–1	4–1	0	20	A/C	6.1	–	17.1	15.54	50.99	3.12	2.58	0.84	0.18	8.01	0.03	98.4	3.7
GERS 4–2	4–2	0	10	A/C	6.7	–	11.9	16.57	53.78	3.44	2.57	0.88	0.20	8.45	0.04	97.8	3.9
	GERS5																
GERS 5–1	5–1	0	15	A	4.1	0.8	28.0	13.55	45.46	2.42	0.55	1.01	0.09	8.11	0.04	99.3	2.4
GERS 5–2	5–2	15	45+	B/C	4.5	–	13.8	18.15	52.02	2.93	0.72	1.14	0.12	9.00	0.04	98.0	2.6
	GERS6					–											
GERS 6–1	6–1	0	8	A	3.3	–	55.7	5.99	29.17	1.21	0.60	0.90	0.03	5.64	0.05	99.3	1.3
GERS 6–2	6–2	8	18	B	3.9	–	18.5	15.19	51.45	2.34	0.19	1.37	0.14	10.32	0.06	99.6	1.7
GERS 6–3	6–3	18	40	B/C	4.4	–	16.0	15.19	51.48	3.15	0.13	1.67	0.24	11.76	0.09	99.8	1.9
GERS 6–4	6–4	40	70+	C	4.7	–	9.5	21.86	53.26	3.15	0.66	1.06	0.14	8.63	0.04	98.3	3.0
	GERS7					–											
GERS 7–1	7–1	0	5	OH	3.3	–	87.2	0.00	7.60	0.18	2.48	0.38	0.00	1.87	0.02	99.7	0.5
GERS 7–2	7–2	5	10	A	3.5	–	25.8	12.03	46.73	1.76	0.85	1.27	0.07	11.13	0.04	99.6	1.4
GERS 7–3	7–3	10	25	B	3.8	–	18.8	17.54	46.53	2.00	0.97	1.35	0.13	10.35	0.05	97.7	1.5
GERS 7–4	7–4	25	50+	C	4.3	–	15.3	18.17	51.31	2.11	1.05	1.23	0.15	10.06	0.04	99.5	1.7
	GERS8																
GERS 8–1	8–1	3	10	A	3.5	0.3	62.5	4.91	21.73	0.76	0.80	1.28	0.02	7.43	0.04	99.5	0.6
GERS 8–2	8–2	10	30	Alu	4.4	–	60.1	10.23	13.82	0.57	0.72	1.03	0.10	12.56	0.03	99.2	0.6
GERS 8–3	8–3	30	55+	Alu/C	4.9	0.4	52.5	13.57	18.34	0.66	1.10	0.98	0.18	11.64	0.03	99.0	0.7
	GERS9																
GERS 9–1	9–1	4	9	A	3.5	–	72.2	3.40	18.91	0.89	0.38	0.51	0.02	2.78	0.04	99.1	1.7
GERS 9–2	9–2	9	17	E	3.4	0.6	28.5	10.22	50.51	2.19	0.07	1.27	0.02	5.60	0.07	98.5	1.7
GERS 9–3	9–3	17	31	Bs	3.6	0.7	16.0	16.47	51.66	2.99	0.13	1.04	0.06	8.89	0.03	97.3	2.9
GERS 11	GERS11	0	50+	A	6.2	–	19.7	12.65	51.42	3.01	4.39	0.86	0.13	7.38	0.04	99.6	3.5

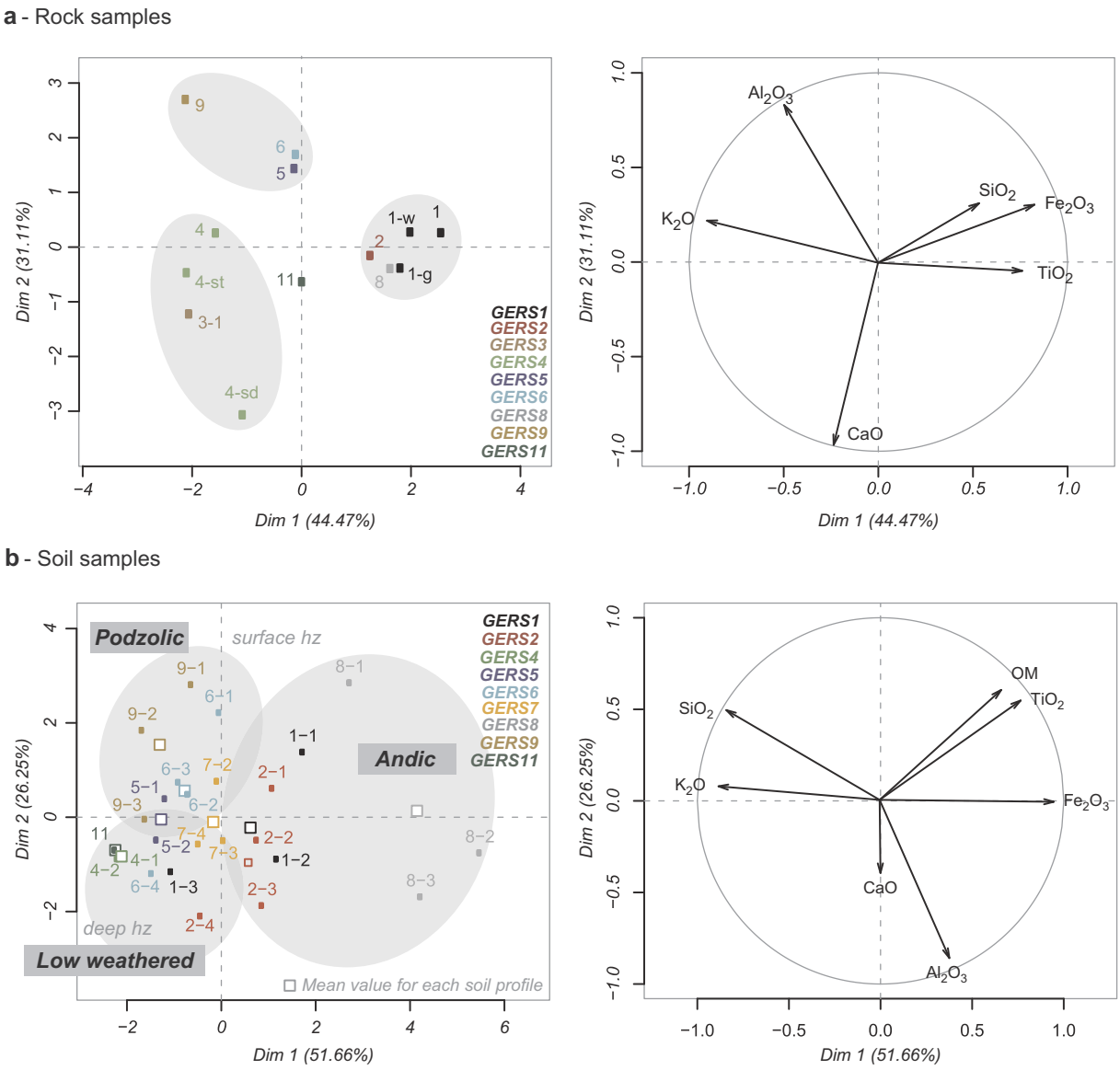

Fig. 3. Biplots of dimensions 1 and 2 and correlation circles of the principal component analysis realized with the rock-parent material of soils (a) and with the soil horizon samples (b).

the main logarithmic trend (reach the secular equilibrium). In the same way, the ^{210}Pbex measures realized in the 9.6–12.5 cm and 12.5–15.5 cm deposits present lower activities and were excluded from the construction of an event-free sedimentary record because they were considered as instantaneous deposits (Arnaud et al., 2002). The depth-corrected plot of ^{210}Pbex activities (*i.e.* depth without instantaneous events) shows two logarithmic relationships providing two mean sedimentation rates: 2.9 ± 0.5 mm·yr^{-1} above 5 cm and 1.3 ± 0.2 mm·yr^{-1} below. Ages were then calculated using the 'constant flux, constant sedimentation rate' (CFCS) model (Goldberg, 1963; Krishnaswamy et al., 1971) applied to the original sediment depth to provide a continuous age-depth relationship.

The ^{137}Cs activity profile (Fig. 4a) has a peak beginning at a depth of 16.5 ± 0.25 cm and reaches a maximum at 13. 5 ± 0.25 cm, interpreted respectively as the beginning of atmospheric production of ^{137}Cs, in 1955 CE due to nuclear weapon test in the Northern Hemisphere and its maximum fallout in 1963 CE (Robbins and Edgington, 1975). The good agreement between the ages of the beginning and maximum artificial radionuclide fallout inferred from the ^{210}Pbex-CFCS model (1952 and 1965) and their known ages (1955 and 1963) supports the validity and the accuracy of our age-depth model in the upper 16 cm of the sediment sequence.

3.3.2. Radiocarbon dating

A total of 10 radiocarbon analyses were performed on selected macrofossils collected from the 5.8-m length of the sediment core (Table 2). These data and those from the short-lived radionuclides measurements were incorporated into Clam to generate the age–depth model of the whole core (Fig. 4b). SacA42472 sample appear too old. It was taken only a few millimeters from an instantaneous deposit. Macrofossils had thus probably been reworked, explaining the age obtained. In consequence, this radiocarbon date was not considered for age–depth modeling. Nevertheless, its high uncertainty, due to its young age, stays in the smooth model computed (Fig. 4b).

The 127 deposits interpreted as instantaneous events represent a total of 163 cm that were removed from the main continuous sedimentation. The remaining 4.2 m of sediment were used to build an event-free sedimentary record (Bøe et al., 2006; Wilhelm et al., 2012). We then calculated an age-depth relationship by a smooth spline interpolation (Fig. 4c). This age-depth model was used to date all

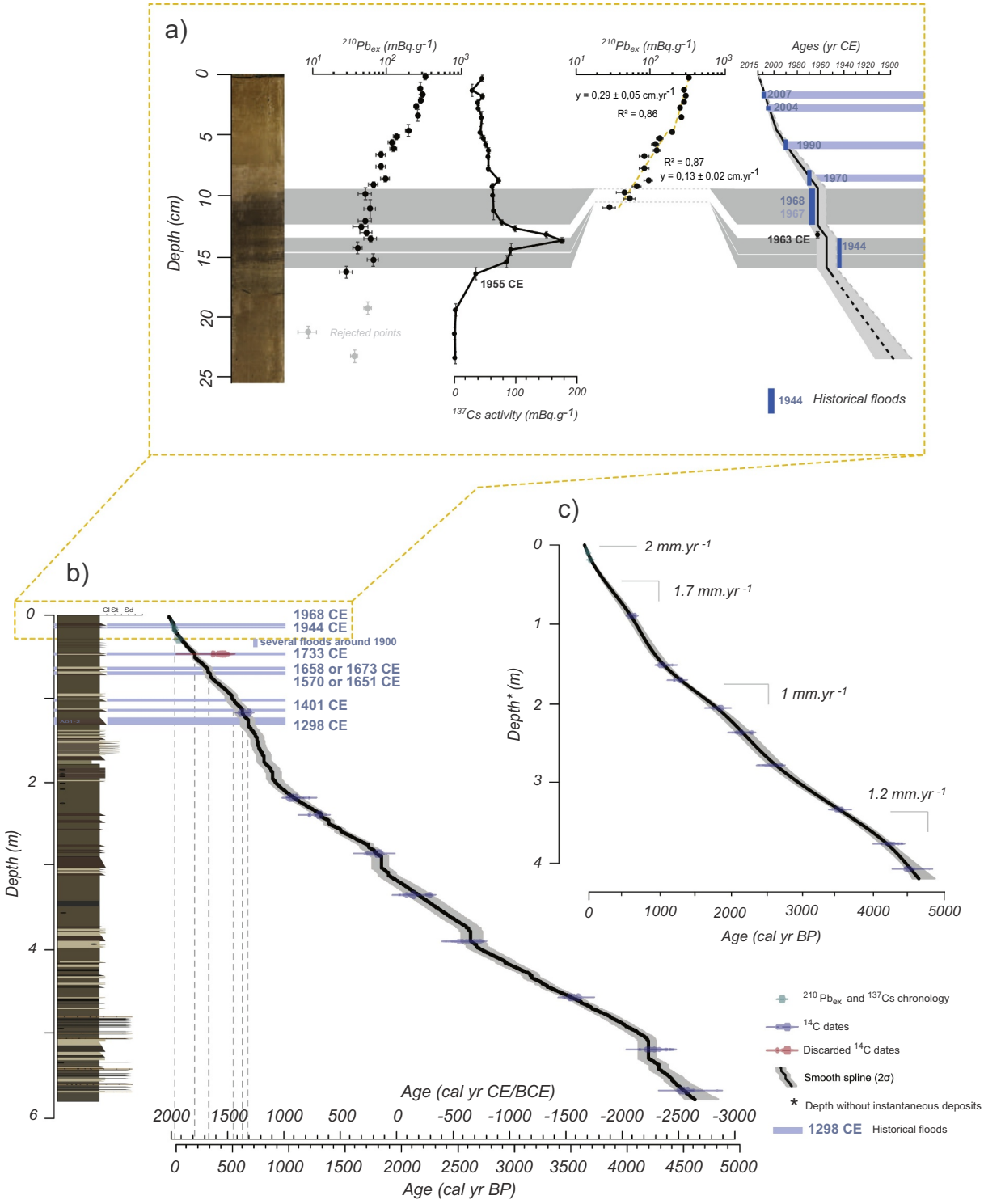

Fig. 4. Age-depth model of Lake Gers sediment sequence including ^{210}Pbex/^{137}Cs chronology (a) and ^{14}C ages (b). Uncertainties are included in the ^{137}Cs activity dots. (c) corresponds to the continuous age-depth model, without instantaneous deposits. Historical floods were collected from Mougin (1914) for the Giffre valley, from RTM online database (http://rtm-onf.ifn.fr) and from municipal documents. CE = Common Era, BCE = Before Common Era.

instantaneous deposits.

The 5.8 m of sedimentary sequence cover the last 4.6 kyr. The sedimentation varies from 0.5 to 2 mm·yr^{-1} with maxima between 4.6 and 4.3 cal kyr BP (1.2 mm·yr^{-1}), 2.5 and 1.9 cal kyr BP (1 mm·yr^{-1}), 900 and 500 cal yr BP (1.7 mm·yr^{-1}) and over the last century (2 mm·yr^{-1}).

3.4. Sedimentary DNA

DNA analyses were performed only in the continuous sedimentation to avoid possible taphonomic biases especially due to grain-size effects that might occurred in instantaneous deposits. Extracellular DNA is expected to be more concentrated in the clayey part than in the sandy/coarse silts part of the flood deposit (Giguet-covex et al., 2019).

The DNA of six mammalian taxa was detected in the sediments of

Table 2
Radiocarbon ages for Lake Gers sediment sequence.

Sample name	Lab. code	Depth (mm)	Sample type	Age (yr BP)	Min. age (cal yr BP)	Max. age (cal yr BP)
GER1	**SacA42472**	**465**	**Herbs, seeds**	**315 ± 30**	**303**	**463**
GER2	SacA42473	1155	Herbs	620 ± 30	552	657
GER3	SacA42474	2180	Bark, herbs	1125 ± 30	960	1172
GER16–1	Poz-81888	2395	Herbs, moss, twigs	1345 ± 30	1186	1308
GER16–2	Poz-81889	2862	Bark, twigs	1885 ± 30	1733	1888
GER16–3	Poz-81890	3347	Wood, bark	2145 ± 30	2009	2303
GER16–4	Poz-81891	3911	Wood, bark	2475 ± 30	2382	2719
GER16–5	Poz-81892	4576	Bark	3270 ± 30	3411	3570
GER16–6	Poz-81894	5206	Twigs, herbs, bark, leaves	3830 ± 35	4100	4405
GER16–7	Poz-81895	5706	Herbs, twigs, bark	4020 ± 35	4418	4570

Bold samples correspond to excluded dates from age-depth modeling.

Lake Gers, specifically *Bos* sp. (cattle), *Canis* sp. (dog/wolf), *Capra* sp. (goat), *Felis* sp. (cat), *Ovis* sp. (sheep) and *Sus* sp. (pig). We only focus on the three taxa associated with grazing activities: *Bos* sp. *Ovis* sp. and *Capra* sp. (Fig. 5a). *Bos* sp. was detected in two samples at 2000 and 1750 cal yr BP, but in only one replicate over eight. It was then recorded in all samples younger than 850 cal yr BP, except in the youngest sample. The highest number of positive PCR replicates was measured at 850, 700 and 400 cal yr BP (3, 6 and 4 positive PCR replicates over 8, respectively, Fig. 5a). *Ovis* DNA was detected in the two samples between 850 and 800 cal yr BP (4 and 5 positive replicates over 8) and in the two samples between 700 and 550 cal yr BP (2 and 1 replicates). *Capra* DNA was detected in two samples between 850 and 750 cal yr BP in 1 or 2 PCR replicates and in the two samples between 400 and 200 cal yr BP in 1 PCR replicates each (Fig. 5a).

For the plants, after the filtering steps, 99 taxa (MOTU) were obtained and classified according to the vegetation stratification and types (*i.e.*, tree layer, shrub layer, herbaceous layer, moss and ferns). We only present in Fig. 5b the tree layer which includes *Prunus*, *Maleae*, *Aquifoliaceae*, *Betulaceae*, *Populus*, *Picea*, *Pinaceae*, *Ulmacea*, *Alnus* and *Acer*. The sample at 4.2 cal kyr BP was removed from our analysis because it contained only 2 taxa detected in 1 or 2 replicates (Apioideaea and Polytrichaceae) any tree sequence, whereas all the other samples older than 1.9 cal kyr BP contain between 15 and 56% of tree DNA sequences (32% in average).

From 4.6 to 1.9 cal kyr BP, the DNA of trees represents 31,5% in average, and 13,5% from 1.9 to the present day (Fig. 5b). During this last period we identified a period of higher tree DNA between 1300 and 900 cal yr BP with 25% in average. The complete sedDNA study combined with pollen analysis of the Lake Gers sediment sequence has been presented by Blanchet et al. (2019) and is subject of a publication in preparation.

4. Discussion

4.1. Source-to-sink dynamics

4.1.1. Pedological origin

PCA for geochemical data from the parent materials (Fig. 3a) highlighted heterogeneity in the geochemistry of Taveyannaz sandstones, especially between the real sandstones characterized by a weathering carbonated aureole found in GERS1, GERS2 and GERS8 and the alternating layer of thick sand and marly levels (GERS3, GERS4). Marly levels were found at lower altitudes than the Taveyannaz sandstones of GERS1, GERS2 and GERS8 (Fig. 1). Considering its colluvial position, GERS11 can be fed by both facies (Figs. 1 and 2). The third main parent material can be associated to glacial deposits in the center (GERS5 and GERS6) and upper part (GERS9) of the catchment (Figs. 1 and 2). PCA from the soil samples defined the same groups as the rock sample PCA, with a distinction for surface and deep horizons. This scheme reflects a strong relation between parent material and soil evolution processes in this catchment. GERS1, GERS2 and GERS8 are affected by andic properties, GERS9, GERS5 GERS6, GERS7 by podzolization and GERS3, GERS4 and GERS11 are low developed and affected by erosion and colluviation. The development of Andosols is rare in the Alps and no Andosols has been described in the French Alps to our knowledge. Their development is possible here from the weathering of Taveyannaz Sandstones which formed from sedimentary deposition of old eroded volcanic complex.

The less weathered soils of Gers catchment and the deepest soil horizons present high K_2O/TiO_2 ratios (Table 1). In the sediments, increases in K_2O/TiO_2 ratios will represent less weathered source inputs (young materials, from regular erosion area), or increasingly deep horizons inputs. Values of K_2O/TiO_2 in the sediments are in the higher range, and beyond what is observed in soils (Fig. 5d and Table 1). In summary, the main sources of sediment are low weathered soils such as GERS11 and GERS4.

Several phases present high contents of OM when K_2O/TiO_2 ratios, erosion and flood deposit frequency are the lowest (Fig. 5). These phases can be interpreted or by slight erosion of soil surface, either as the expression of lacustrine OM that is less diluted than during the periods of higher terrigenous inputs. Between 900 and 800 cal yr BP, the increase in OM may be also link to grazing on the delta of the lake, which could have bring lots of organic matter from dungs.

4.1.2. Flood chronicle

Normally graded deposits are common features in lake sediments. There are commonly associated to turbidity currents triggered by mass movements or by flood events. To verify this hypothesis, we compared our record with the historical flood calendar of the downstream Giffre river established by Mougin (1914) and completed by local archives and internet database of RTM (ONF-RTM database, http://rtm-onf.ifn.fr). The comparison allows to associate the thickest deposits to historical floods from 1298 CE to today (Table 3). The proposed dates fitted within 20 years in average, throughout the last 650 years. Only three deposits dated at 513 cal yr BP could not be identified in the historical archives, possibly due to both their low thicknesses and their old age (Table 3). This good correspondence supports both the assumption of the torrential origin of these deposits and the chronology of the sequence for this period.

The frequency of the instantaneous deposits was estimated for a period of 101 years (Fig. 5e). Sandy levels are presented in a different color as they can have a different origin from the other events and are only present from 4.6 to 3.8 cal yr BP (Fig. 5e). Sandy levels occur from 2 to 10 deposits per 101 years on this period, with three higher frequency periods around 4.4, 4.15 and 3.9 cal kyr BP. The frequency of the other deposits ranges from 0 to 33 events (Fig. 5e). The centennial frequency ranges from 0 to 4 between 4.6 and 2.7 cal kyr BP, with up to 4 events from 4.6 to 4.15, 3.7 to 3.5, 3.3 to 3.1 and 2.95 to 2.85 cal kyr BP. The frequency reaches 8 events per 101 years between 2.7 and 2.5 cal kyr BP before a period where no events were recorded between 2.5 and 1.95 cal kyr BP. The frequency reaches up to 4 events again from 1.95 to 1.65 cal kyr BP and up to 2 events between 1.5 and

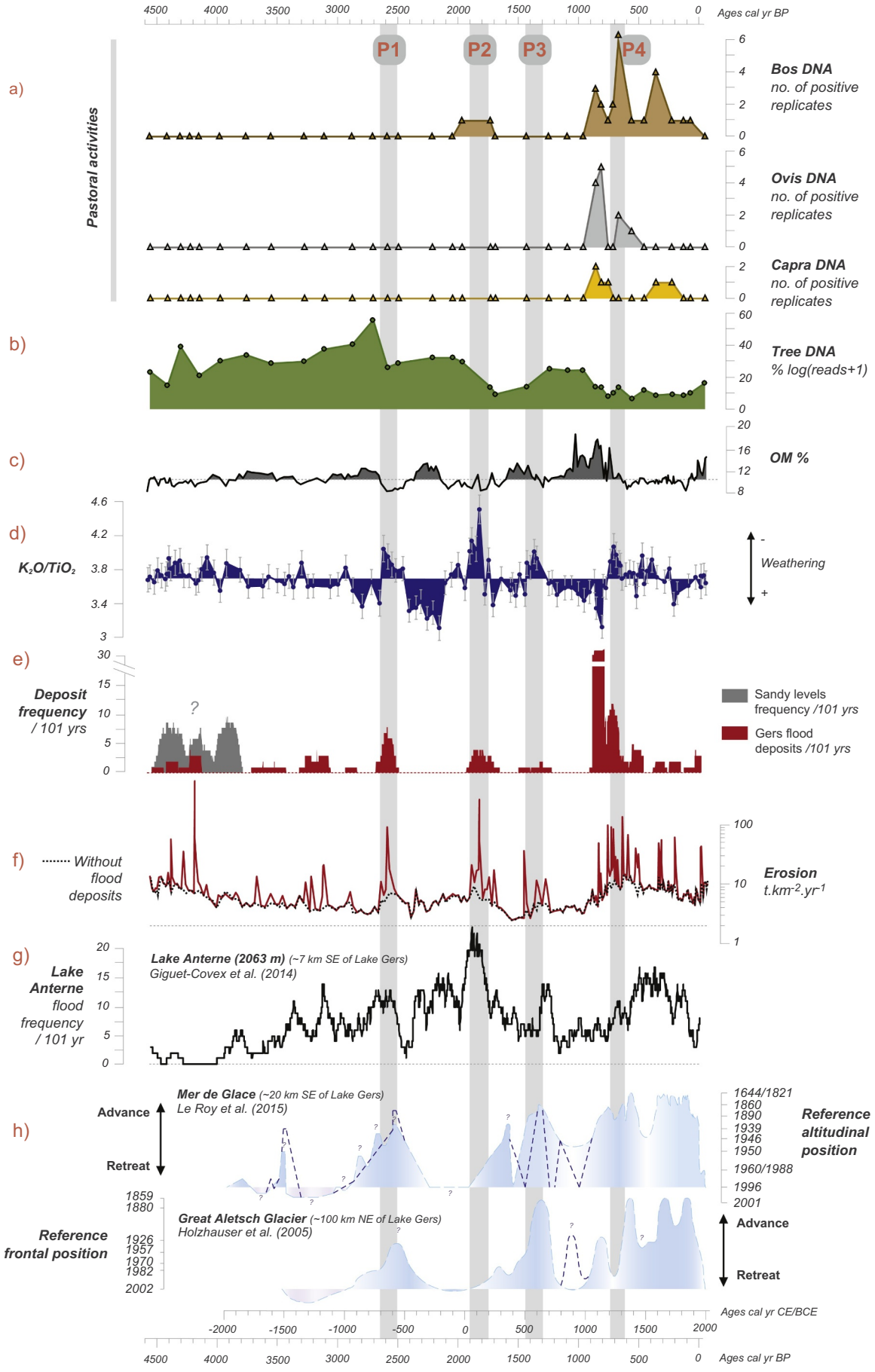

(caption on next page)

Fig. 5. Evolution of agro-pastoral activities, vegetation and erosion in the Lake Gers catchment during the late Holocene as inferred from mammal DNA, including DNA of cow, sheep and goat (a), tree DNA (b), organic matter (OM) content (c), K_2O/TiO_2 ratio (d) measured in the continuous sedimentation, the centennial deposit frequency in Lake Gers (e), erosion in Lake Gers catchment (f), compared to Lake Anterne centennial flood frequency (g) and regional glacier records (h) from Le Roy et al. (2015) and Holzhauser et al. (2005) as climate proxies.

1.23 cal kyr BP. The maximum frequency occurs from 900 to 670 cal yr BP with up to 33 events between 900 and 800 cal yr BP (Fig. 5e). The frequency stays between 2 and 4 events per 101 yrs until 460 cal yr BP, then between 0 and 2 until the last century.

The origin of sandy deposits between 4.6 and 3.8 cal kyr BP is not solved. As two of them are associated to a graded layer, a flood deposit is possible, but can also be due to chance, *i.e.*, a sand deposit followed by a flood deposit. No other proxies analyzed in the sediment core provide information about the disappearance of these deposits after 3.8 cal kyr BP. They correspond to another source which is no longer mobilized or which does not reach the lake since 3.8 kyr. They happen while very low flood-frequency and erosion are recorded at Lake Anterne (Fig. 5g). 3.8 kyr is also considered as a major paleohydrological transition toward wetter regional conditions as evidenced by different studies in the Alps (Nicolussi et al., 2005; Magny et al., 2011; Arnaud et al., 2012; Le Roy et al., 2015; Arnaud et al., 2016; Rapuc et al., 2019). This change in the sedimentary dynamic could be a consequence of the 4.2 kyr event recognized in different types of archives at many global locations. The avalanches that arrive on the lake can also bring sands when ice is melting, especially from the Taveyannaz sandstones cliff above (Fig. 1c). However, they appear to have a constant gran-size, while avalanches bring very different grain-size materials (weak sorting), and usually even coarse (*e.g.*, gravels, pebbles) with dropstones in lake sediments (Fouinat et al., 2017b).

4.1.3. Long-term erosion

Erosion was first calculated without the instantaneous deposits (Fig. 5f, dotted line), and then including each instantaneous deposit (Fig. 5f). Erosion is approximately 10 $t{\cdot}km^{-2}{\cdot}yr^{-1}$ between 4.6 and 4.1 cal kyr BP, with three highest peaks at 30, 50 and 200 $t{\cdot}km^{2}.an^{-1}$ during the years of instantaneous deposits. Erosion decrease at approximately 4–5 to 3 $t.km^{-2}{\cdot}yr^{-1}$ from 4.1 to 2.6 cal kyr BP, with punctual event induced-erosion peaks until 20 $t{\cdot}km^{2}{\cdot}an^{-1}$. Erosion increases at 9 $t{\cdot}km^{-2}{\cdot}yr^{-1}$ between 2.6 and 1.7 cal kyr BP, with two highest periods from 2.6 to 2.5 and 1.9 to 1.7 cal yr BP. Erosion is lower from 1700 to 950 cal yr BP except during the higher event frequency period from 1.4 to 1.3 cal kyr BP (Fig. 5e, f). Erosion increases up to 15 $t{\cdot}km^{-2}{\cdot}yr^{-1}$ outside flood deposits and up to 100 $t{\cdot}km^{-2}{\cdot}yr^{-1}$ with flood deposits between 950 and 600 cal yr BP, and slightly decreases from 600 to 0 cal yr BP. The last 65 yrs are characterized by an increase erosion trend.

The calculation of erosion is very simplified and absolute values are to be carefully used. Nevertheless, they are in the order of magnitude of erosion modeled and recorded in Europe (Enters et al., 2008; Cerdan et al., 2010; Egli et al., 2014; Vanmaercke et al., 2015). Furthermore, Bajard et al., 2017a showed that the uncertainty of the volume of sediment weakly influenced the amount of erosion. Otherwise, with instantaneous inputs from floods, the erosion triggered at each of these deposits is very depending of the deposit time of the considered "sample depth" below. Without considered the flood inputs, erosion is still higher during higher flood-frequency periods, suggesting an impact of these events on the continuous sedimentation. For example, a part of the material mobilized during an extreme event can be stocked in the catchment before being remobilized with later rainfall. This assumption is strongly supported by the variation of K_2O/TiO_2 that displays always higher values during high flood-frequency periods (Fig. 5d, e).

4.2. Environmental dynamics and agro-pastoral activities in the late Holocene

In the Northwestern Alps, first important developments of pastures happened after 3600 to 3000 cal yr BP. In the Anterne mountain (Fig. 1e), palynological studies from Survilly and Ecuelles peat bogs show an expansion of Alnus around 3600 and 3000 cal yr BP respectively, and were associated to clear-cutting and grazing activities (David, 2010a,b). Archaeological evidences found close to Lake Anterne confirms, with sedDNA from the lake, the long livestock farming history of this area (Rey, 2008, 2010; Giguet-Covex et al., 2014). Similar observations were made in the Swiss Alps from Lake Sägitalsee at 1935 m a.s.l. (Wick et al., 2003). It is also during this same period that first human clearing and grazing activities were identified in the area of the Petit Saint Bernard pass (2188 m a.s.l, French-Italian border), by independent palynological, DNA, pedoanthracological and archaeological studies (Talon, 2006; Rey et al., 2008; Bajard et al., 2017b).

At lake Gers, the period between 4600 and 2700 cal yr BP is characterized by no or low variations of the geochemistry with four periods of low flood-frequency, reflecting constant inputs and slight evolution in the landscape. The catchment was rather forested. No pasture activity was recorded by DNA. At 2700 cal yr BP, the peak in tree DNA (Fig. 5b) is mainly due to Alnus (data not shown). This occurrence of Alnus, could reflect first development of grazing in lake Gers catchment.

After 2700 cal yr BP, both OM contents and K_2O/TiO_2 ratio present higher variations, mainly anticorrelated. The four phases of higher K_2O/TiO_2 ratio (noted P1 to P4, Fig. 5), reflecting the contribution of less weathered materials are associated to higher flood-frequency periods. They appear as ruptures in the evolution of the landscape. Floods had to disrupt the catchment bringing less weathered materials from rejuvenated soils through erosion and colluviation movements, while outside periods of higher flood-frequency, the continuous sedimentation reflected the low erosion of surface soils, with higher OM contents and higher weathered materials.

The Roman period is marked a slight decrease of DNA of trees and the first occurrence of cow DNA in the sediments between 2000 and 1700 cal yr BP, suggesting deforestation and development of cattle grazing in the catchment. The rejuvenation of soils between 1900 and 1750 cal yr BP (P2 phase) is associated with this development of grazing activities. On the other hand, cow and bos DNA were detected earlier in the sediments of Lake Anterne (Fig. 1e), between 2400 and 1900 cal yr BP (Giguet-Covex et al., 2014). This difference could reflect a development of pastoral areas by the areas at higher altitudes.

Between 1300 and 900 cal yr BP, a recovery in the forest restored surface soil inputs. No flood deposit was recorded during this period. A similar recolonization of the vegetation was recorded at Lake Verney (2088 m) in the Petit Saint Bernard pass area (French-Italian border), approximately at the same period with evidence of a slight recovery in the podzolic processes in the catchment (Bajard et al., 2017b). The origins of this decrease in pastoral activities could therefore be more global (*e.g.*, climate forcing).

After 950 cal yr BP, cattle grazing activities seems to be continuous. Sheep and goat were present especially until 800 cal yr BP. The Gers valley is known to be one of the main route to bring animals to the Sales Vallon (Fig. 1e), which is another pasture located a few kilometers away (Guffond and Mélo, 2018). At Sales, 84 archaeological structures and remains of building were identified (Guffond, 2017). Two animal bones, buried in the buildings, were dated 865 and 675 yr BP. They independently confirm the medieval implantation of these mountains.

Table 3
Comparison of flood deposits recorded in Lake Gers sediments with historical floods of the Giffre River for the last 650 yrs. CE = Common Era.

Flood thickness (cm)	Age cal. BP	Age cal. CE	min CE	Max CE	Historical flood	Age difference (yrs)	Reference	Historical document
3	−14	1964	1971	1956	1968	4	RTM archives	
1	−6	1956	1964	1947	1944	12	Municipal archives (Sixt-Fer à Cheval)	
1	−6	1959	1964	1947	1944	12	Municipal archives (Sixt-Fer à Cheval)	
0.5	79	1871	1890	1856	1878	7	Mougin (1914)	Patriote Savoisien, 1878, 2 juin, 21 juin, 4 septembre
1.5	204	1746	1776	1716	1733	13	Mougin (1914)	Arch. Dép. H.-S. T. P. Fy. Liasses anciennes, 14 juin 1737, n°236
2.5	204	1746	1776	1716	1733	13	Mougin (1914)	Arch. Dép. H.-S. T. P. Fy. Liasses anciennes, 14 juin 1737, n°236
3.5	318	1632	1672	1593	1658 or 1673	26 or 41	Mougin (1914)	Revue savoisienne, 1898. Gonthier. Eboulements historiques.
3.5	338	1612	1654	1572	1570 or 1651	46 or 39	Mougin (1914)	Revue savoisienne, 1898. Gonthier. Eboulements historiques.
1	513	1437	1490	1390	?	–	–	
1	513	1437	1490	1390	?	–	–	
1	513	1437	1490	1390	?	–	–	
2	534	1416	1470	1369	1401?	15	Mougin (1914)	Acad. Sallès Tome XX. Abbé Feige. Monographie de Mélan.
5	595	1355	1409	1307	1401?	46	Mougin (1914)	Acad. Sallès Tome XX. Abbé Feige. Monographie de Mélan.
11	641	1309	1364	1258	1298	11	Mougin (1914)	Acad. Sallès Tome XX. Abbé Feige. Monographie de Mélan.

Moreover, the intensification of agricultural activities in this part of the Alps in the medieval period was also reflected by the expansion and opening of new grazing areas like at Bénit, a pasture located 18 km west of Gers (Bajard et al., 2018).

This diversification of the pastoral activities was associated with the expansion of pastoral areas, as suggested by the decrease in the DNA of trees and increase in erosion of OM-rich and highly weathered soils associated with the high frequency of thin flood deposits. They suggest a progressive erosion of soils, from weathered and organic surface horizons to deep, less weathered horizons (P4 phase), leading to a more important development of Cambisols, instead of Podzols and Andosols. From 700 cal yr BP to the present, few changes were recorded except the relative decrease in flood-frequency, suggesting a stabilization of the landscape. Historical documents from 1418 CE (532 yr cal BP) attests that animals and heifers were bring to Sales Vallon (Guffond and Mélo, 2018). In 1847, 300 cows were grazing below Pointe Pelouse.

4.3. Impact of climate and human in the subalpine area

4.3.1. Erosion and climate patterns at the local scale

For both the Roman and medieval periods (P2 and P4 phases, Fig. 5), the increases in erosion, flood-frequency and K_2O/TiO_2 ratio appear to be mostly due to human activities. For the two other periods (P1 and P3 phases), the impact of human activities could be under-recorded, especially at the early beginning of the deforestation process. Changes in vegetation may be partly masked in the first hundred years after landscape modifications, as DNA may be stored in soils, and will only be transferred to the lake with erosion (Parducci et al., 2017; Giguet-covex et al., 2019). The extreme values of K_2O/TiO_2 ratio and the highest flood-frequency recorded in the same way than during P2 and P4 phases constitute one more argument in the assumption of human induced flood-frequency increase in P1 and P3 phases, considering that roman and medieval periods were the main periods of pastoral activities in the Alps.

In order to verify this hypothesis, we compared the Lake Gers record with regional glacier records (Fig. 5h). Holzhauser et al. (2005) and Le Roy et al. (2015) provide reconstitutions of the dynamics of the Great Aletsch Glacier (100 km northeast of Lake Gers) and of the Mer de Glace (20 km southeast of Lake Gers), respectively, throughout the last 3500 yrs. Both P1 and P3 phases are synchronous with glacier advances of both glaciers, suggesting mainly a climate cooling to explain the higher flood-frequency periods and the associated erosion increases. Around the Alps, Arnaud et al. (2016) pointed out that colder periods generally favor higher flood frequency. Indeed, a climate cooling could affect vegetation by reducing its development. But vegetation protects soils from erosion, and soils also absorb precipitation, limiting run off and flooding. So, a cooling of the climate could increase flood events.

The P4 phase but also all the last millennia of Lake Gers sedimentary record is also largely associated to glacier fluctuations. The P4 phase could thus be associated to both climate and human forcings. Both effects of substantial land-use and precipitation patterns changes could be responsible for the higher flood-frequency recorded at the beginning of the last millennia.

In order to draw the regional pattern of erosion we compared the Lake Gers record with Lake Anterne sedimentary record (7 km southward). At Anterne, both the flood-frequency and sedimentation rate, which present the same variations, were used as proxies of erosion (Giguet-Covex et al., 2011, 2012), as observed in Lake Gers sequence. Higher flood-frequency was recorded at Lake Anterne (max 24/101 yrs, 7/101 yrs on average) than at Lake Gers (max 33/101 yrs, 2/101 yrs in average). The catchment of Lake Anterne is possibly more susceptible to flood because of both its higher altitude (*e.g.*, difference in vegetation, precipitations and snow melting) and the highest erodibility of the schists, which mainly cover its catchment. Pastoral activities at Anterne were recorded mainly from 2400 to 1900 cal yr BP (cow and sheep) and from 1000 to 200 cal yr BP (mainly cow) (Giguet-Covex et al., 2014).

The effects of human activities seem to be more marked at Anterne during the late Iron age and the beginning of roman period, with both cow and sheep grazing, associated with maximum of erosion, while this period is much more weakly marked by human activities at Lake Gers (Fig. 5).

The erosion recorded in both lakes display similar variations, especially between 3200 and 1000 cal yr BP. After 1000 cal yr BP, both erosion patterns seem more different. At Lake Anterne, erosion increases slightly, and more after 500 cal yr BP in relation with wetter and colder climate conditions of the Little Ice Age (Giguet-Covex et al., 2012). At Lake Gers, erosion was very important after 950 cal yr BP, in relation with human activities, triggering a high destabilization of soils and an increase of flood deposits. Erosion trajectories of soils in both catchments are similar while human impact is moderated, as noticed in the Roman period, and then differ when human pressure strengthens in the Middle Age. This comparison suggests that from the medieval period, human activities overwhelm the impact of climate on erosion in Lake Gers catchment. A similar observation was realized from Lake La Thuile sediment sequence for the same period (Bajard et al., 2016). Both erosion and soil disruption were triggered first by climate forcing (*i.e.*, heavy precipitations, snow cover duration) and strongly increase according to the intensity of human activities that disrupt soils and make them more easily erodible. However, changes in hydrological patterns could be more associated to bare soils than change in vegetation (Cosandey et al., 2005). Such an increase in the erodibility of a catchment with anthropic activities was also recorded in the southern Alps and represent a major threat for the future (Brisset et al., 2017).

4.3.2. Consequences of land use modifications on the vulnerability to climate changes

Long-term changes in land use has led to an increase in transport capacity of water in the catchment (*e.g.* increased of Hortonian flow due to vegetation changes or compaction) and increase in the sediment supply through the erosion initiated by grazing activities and deforestation. These consequences trigger an input of water and sediments more important to downstream areas where human activities take place. In interaction with climate changes and multiplication of extreme events, these consequences increase the vulnerability of population to flood hazards. Therefore, upstream areas should be more taken into account in the adaptation to climate change and risk prevention plans.

Effect of floods, favored by human-induced land-use changes increases losses of soils and their associated ecosystem services. Anthropogenic land-use changes are known to be an important way to lose organic carbon (Carcaillet et al., 2002; Kaplan et al., 2011). However, human activities induced-erosion is not well considered in the assessment of organic C losses and in the global C budget (Lal, 2003). Erosion could yet accelerate organic C losses in the atmosphere, by mineralization to CO_2, and strengthen climate warming (Alewell et al., 2009; Wang et al., 2017). The less important OM content in the sediment of Lake Gers (10% in average) than in soils of the catchment (30% in average, Table 1) suggests a loss of organic carbon with erosion. However, our data do not allow to assess the location of mineralization, during transport or within the lake. As a result, a larger consideration and management of upstream areas would reduce the vulnerability of population downstream to flood events and participate to carbon storage to limit the global warming.

5. Conclusions

The sediment sequence of Lake Gers (1540 m a.s.l.) in the Northern French Alps provides a continuous record of environmental changes throughout the last 4.6 kyr. The sequence is punctuated by 127 instantaneous deposits, including 93 graded deposits identified as flood deposits. The other deposits are sand layers occurring only from 4.6 to 3.8 cal kyr BP, whose origin was not determined. Multiproxy analyses of the continuous sedimentation, including geochemistry, loss on ignition and DNA analyses, were compared to flood-frequency and to current soils of the catchment. Erosion was quantified from the lake filling, including flood events and compared to regional climate and erosion records.

Three potential geochemical sources were identified in the catchment, corresponding to variations in geological formations over which different pedogenetic processes were associated, *i.e.*, Podzolization, Andosolization and colluviation. Colluviation and low weathered material seem to be responsible for the main inputs in the lake. Podzols and Andosols features were not identified in the sediment with our analyses.

Four phases of decrease in the weathering of sedimentary inputs were associated to higher flood-frequency periods, suggesting the progressive erosion of soils and their periodic destabilization and rejuvenation. Two of the four weathering decrease phases (*i.e.* increase in K_2O/TiO_2 ratio) were associated with climate cooling in the 2650–2500 and 1450–1300 cal yr BP periods. The two other phases were associated with human activities, *i.e.* deforestation and pastoralism, during the late Roman period and in the Middle Age, mainly with cow grazing. In the last millennia, agricultural activities are diversified with sheep and goats, and combined to climate forcing. Both effects, agriculture and climate, triggered an even higher flood-frequency deposit and higher erosion. This last anthropic phase evidenced higher modifications operated by agro-pastoral activities in the catchment (*e.g.*, vegetation) and a higher sensibility to climate events.

Declaration of competing interest

The authors do not declare any conflict of interest in the publication of this research.

Acknowledgments

The authors thank the municipality of Samoens for access and coring authorizations to Lake Gers, and the ski resort of Flaine - Grand Massif for the winter access to the lake by the ski slopes (Malvina Sculo, ski patrols and snow groomer driver). Thanks to Jim Félix-Faure, Laurent Fouinat and Anouk Leloup-Besson for field support and Dominique Navillod for her welcome to the “Gite de Gers”. Thanks also to Sarah Bureau for ICP-AES analyses at ISTerre laboratory. 14C analyses were acquired thanks to the CNRS-INSU ARTEMIS national radiocarbon AMS measurement program at Laboratoire de Mesure du 14C (LMC14) in the CEA Institute at Saclay (French Atomic Energy Commission). The authors thank also the Laboratoire Souterrain de Modane (LSM) facilities for the gamma spectrometry measurements. DNA analyses were supported by AGIR-PAGE Euromont 2016 project. We thank Morgan T. Jones for correcting the English of the article and the two anonymous reviewers for advice in improving our manuscript.

Data availability

Datasets related to this article can be found at https://data.mendeley.com/datasets/j9x7yhcvd4/draft?a=1fbbfa5b-b76e-4d5b-b428-adc496d7c2d4, (doi:10.17632/j9x7yhcvd4.1) an open-source online data repository hosted at Mendeley Data ([CITATION TO DATASET]).

Appendix A. Supplementary data

Supplementary data to this article can be found online at https://doi.org/10.1016/j.palaeo.2019.109462.

References

Adhikari, K., Hartemink, A.E., 2016. Linking soils to ecosystem services — a global

review. Geoderma 262, 101–111. https://doi.org/10.1016/j.geoderma.2015.08.009.
Alewell, C., Schaub, M., Conen, F., 2009. A method to detect soil carbon degradation during soil erosion. Biogeosci. Discuss. 6, 5771–5787. https://doi.org/10.5194/bgd-6-5771-2009.
Appleby, P., Richardson, N., Nolan, P., 1991. 241Am dating of lake sediments. In: Environmental History and Palaeolimnology. Springer, pp. 35–42.
Arnaud, F., Lignier, V., Revel, M., Desmet, M., Beck, C., Pourchet, M., Charlet, F., Trentesaux, A., Tribovillard, N., 2002. Flood and earthquake disturbance of 210Pb geochronology (Lake Anterne, NW Alps). Terra Nova 14, 225–232.
Arnaud, F., Révillon, S., Debret, M., Revel, M., Chapron, E., Jacob, J., Giguet-Covex, C., Poulenard, J., Magny, M., 2012. Lake Bourget regional erosion patterns reconstruction reveals Holocene NW European Alps soil evolution and paleohydrology. Quat. Sci. Rev. 51, 81–92. https://doi.org/10.1016/j.quascirev.2012.07.025.
Arnaud, F., Poulenard, J., Giguet-Covex, C., Wilhelm, B., Révillon, S., Jenny, J.-P., Revel, M., Enters, D., Bajard, M., Fouinat, L., et al., 2016. Erosion under climate and human pressures: an alpine lake sediment perspective. Quat. Sci. Rev. 152, 1–18.
Bailey, R.W., Becraft, R.J., Forsling, C.L., 1934. Floods and Accelerated Erosion in Northern Utah. US Government Printing Office.
Bajard, M., Sabatier, P., David, F., Develle, A.-L., Reyss, J.-L., Fanget, B., Malet, E., Arnaud, D., Augustin, L., Crouzet, C., Poulenard, J., Arnaud, F., 2016. Erosion record in Lake La Thuile sediments (Prealps, France): evidence of montane landscape dynamics throughout the Holocene. The Holocene 26, 350–364.
Bajard, M., Poulenard, J., Sabatier, P., Develle, A.-L., Giguet-Covex, C., Jacob, J., Crouzet, C., David, F., Pignol, C., Arnaud, F., 2017a. Progressive and regressive soil evolution phases in the Anthropocene. CATENA 150, 39–52. https://doi.org/10.1016/j.catena.2016.11.001.
Bajard, M., Poulenard, J., Sabatier, P., Etienne, D., Ficetola, F., Chen, W., Gielly, L., Taberlet, P., Develle, A.-L., Rey, P.-J., Moulin, B., Beaulieu, J.-L. de, Arnaud, F., 2017b. Long-term changes in alpine pedogenetic processes: effect of millennial agro-pastoralism activities (French-Italian Alps). Geoderma 306, 217–236. https://doi.org/10.1016/j.geoderma.2017.07.005.
Bajard, M., Etienne, D., Quinsac, S., Dambrine, E., Sabatier, P., Frossard, V., Gaillard, J., Develle, A.-L., Poulenard, J., Arnaud, F., Dorioz, J.-M., 2018. Legacy of early anthropogenic effects on recent lake eutrophication (Lake Bénit, northern French Alps). Anthropocene 24, 72–87. https://doi.org/10.1016/j.ancene.2018.11.005.
Blaauw, M., 2010. Methods and code for 'classical' age-modelling of radiocarbon sequences. Quat. Geochronol. 5, 512–518. https://doi.org/10.1016/j.quageo.2010.01.002.
Blanchet, C., Giguet-Covex, C., Blanchet, C., Giguet-Covex, C., Messager, E., Etienne, D., Gielly, L., Ficetola Gentile, F., Poulenard, J., Bajard, M., Sabatier, P., Arnaud, F., 2019. Vegetation history of the lake Gers (Northern French Alps) told by two different narrators: pollen and DNA. In: 20th Congress of the International Union for Quaternary Research (INQUA).
Bøe, A.-G., Dahl, S.O., Lie, Ø., Nesje, A., 2006. Holocene river floods in the upper Glomma catchment, southern Norway: a high-resolution multiproxy record from lacustrine sediments. The Holocene 16, 445–455. https://doi.org/10.1191/0959683606hl940rp.
Boyer, F., Mercier, C., Bonin, A., Le Bras, Y., Taberlet, P., Coissac, E., 2016. obitools: a unix-inspired software package for DNA metabarcoding. Mol. Ecol. Resour. 16, 176–182.
Brisset, E., Guiter, F., Miramont, C., Troussier, T., Sabatier, P., Poher, Y., Cartier, R., Arnaud, F., Malet, E., Anthony, E.J., 2017. The overlooked human influence in historic and prehistoric floods in the European Alps. Geology 45, 347–350. https://doi.org/10.1130/G38498.1.
Carcaillet, C., Almquist, H., Asnong, H., Bradshaw, R., Carrion, J., Gaillard, M.-J., Gajewski, K., Haas, J., Haberle, S., Hadorn, P., et al., 2002. Holocene biomass burning and global dynamics of the carbon cycle. Chemosphere 49, 845–863.
Cerdan, O., Govers, G., Le Bissonnais, Y., Van Oost, K., Poesen, J., Saby, N., Gobin, A., Vacca, A., Quinton, J., Auerswald, K., Klik, A., Kwaad, F.J.P.M., Raclot, D., Ionita, I., Rejman, J., Rousseva, S., Muxart, T., Roxo, M.J., Dostal, T., 2010. Rates and spatial variations of soil erosion in Europe: a study based on erosion plot data. Geomorphology 122, 167–177. https://doi.org/10.1016/j.geomorph.2010.06.011.
Cosandey, C., Andréassian, V., Martin, C., Didon-Lescot, J.F., Lavabre, J., Folton, N., Mathys, N., Richard, D., 2005. The hydrological impact of the Mediterranean forest: a review of French research. J. Hydrol. 301, 235–249. https://doi.org/10.1016/j.jhydrol.2004.06.040.
Daily, G.C., Matson, P.A., Vitousek, P.M., 1997. Ecosystem services supplied by soil. In: Nature's Services: Societal Dependence on Natural Ecosystems, pp. 113–132.
David, F., 2010a. An example of the consequences of human activities on the evolution of subalpine landscapes. C.R. Palevol 9, 229–235. https://doi.org/10.1016/j.crpv.2010.06.002.
David, F., 2010b. Expansion of green alder (Alnus alnobetula [Ehrh] K. Koch) in the northern French Alps: a palaeoecological point of view. C. R. Biol. 333, 424–428. https://doi.org/10.1016/j.crvi.2010.01.002.
Doyen, E., Etienne, D., 2017. Ecological and human land-use indicator value of fungal spore morphotypes and assemblages. Veg. Hist. Archaeobotany 26, 357–367. https://doi.org/10.1007/s00334-016-0599-2.
Egli, M., Dahms, D., Norton, K., 2014. Soil formation rates on silicate parent material in alpine environments: different approaches–different results? Geoderma 213, 320–333. https://doi.org/10.1016/j.geoderma.2013.08.016.
Enters, D., Dorfler, W., Zolitschka, B., 2008. Historical soil erosion and land-use change during the last two millennia recorded in lake sediments of Frickenhauser See, northern Bavaria, central Germany. The Holocene 18, 243–254. https://doi.org/10.1177/0959683607086762.
Ewing, H.A., Nater, E.A., 2002. Holocene soil development on till and outwash inferred from lake-sediment geochemistry in Michigan and Wisconsin. Quat. Res. 57, 234–243. https://doi.org/10.1006/qres.2001.2303.
FAO (Ed.), 2006. Guidelines for Soil Description, 4 [rev.] ed. FAO, Rome.
Fouinat, L., Sabatier, P., Poulenard, J., Etienne, D., Crouzet, C., Develle, A.-L., Doyen, E., Malet, E., Reyss, J.-L., Sagot, C., Bonet, R., Arnaud, F., 2017a. One thousand seven hundred years of interaction between glacial activity and flood frequency in proglacial Lake Muzelle (western French Alps). Quat. Res. 87, 407–422. https://doi.org/10.1017/qua.2017.18.
Fouinat, L., Sabatier, P., Poulenard, J., Reyss, J.-L., Montet, X., Arnaud, F., 2017b. A new CT scan methodology to characterize a small aggregation gravel clast contained in a soft sediment matrix. Earth Surf. Dyn. 5, 199–209. https://doi.org/10.5194/esurf-5-199-2017.
Giguet-Covex, C., Arnaud, F., Poulenard, J., Disnar, J.-R., Delhon, C., Francus, P., David, F., Enters, D., Rey, P.-J., Delannoy, J.-J., 2011. Changes in erosion patterns during the Holocene in a currently treeless subalpine catchment inferred from lake sediment geochemistry (Lake Anterne, 2063 m a.s.l., NW French Alps): the role of climate and human activities. The Holocene 21, 651–665. https://doi.org/10.1177/0959683610391320.
Giguet-Covex, C., Arnaud, F., Enters, D., Poulenard, J., Millet, L., Francus, P., David, F., Rey, P.-J., Wilhelm, B., Delannoy, J.-J., 2012. Frequency and intensity of high-altitude floods over the last 3.5ka in northwestern French Alps (Lake Anterne). Quat. Res. 77, 12–22. https://doi.org/10.1016/j.yqres.2011.11.003.
Giguet-Covex, C., Pansu, J., Arnaud, F., Rey, P.-J., Griggo, C., Gielly, L., Domaizon, I., Coissac, E., David, F., Choler, P., Poulenard, J., Taberlet, P., 2014. Long livestock farming history and human landscape shaping revealed by lake sediment DNA. Nat. Commun. 5. https://doi.org/10.1038/ncomms4211.
Giguet-covex, C., Ficetola, F.G., Walsh, K.J., Poulenard, J., Bajard, M., Fouinat, L., Pierre, S., Gielly, L., Messager, E., Develle, A.-L., David, F., Taberlet, P., Brisset, E., Guiter, F., Sinet, R., Fabien, A., 2019. New insights on lake sediment DNA from the catchment: importance of taphonomic and analytical issues on the record quality (preprint). EarthArXiv. https://doi.org/10.31223/osf.io/cnh3r.
Giorgi, F., Torma, C., Coppola, E., Ban, N., Schär, C., Somot, S., 2016. Enhanced summer convective rainfall at Alpine high elevations in response to climate warming. Nat. Geosci. 9, 584–589. https://doi.org/10.1038/ngeo2761.
Goldberg, E.D., 1963. Geochronology with 210Pb. In: Radioactive Dating, pp. 121–131.
Guffond, C., 2017. Sixt-Fer-à-Cheval (Haute-Savoie). Alpage de Sales. Archéologie Médiévale 180.
Guffond, C., Mélo, A., 2018. Une institution collective dans l'histoire: l'alpage de Sales (Sixt-Fer-à-Cheval, Haute-Savoie, fin XIVe-fin XIXe siècles). In: Etat et institutions en Savoie - Actes du 46e Cong. des Soc. Sav. de Savoie - 2016. 2018. Soc. d'Hist. et d'Archéologie de Maurienne, pp. 253–266.
Heiri, O., Lotter, A.F., Lemcke, G., 2001. Loss on ignition as a method for estimating organic and carbonate content in sediments: reproducibility and comparability of results. J. Paleolimnol. 25, 101–110.
Holzhauser, H., Magny, M.J., Zumbühl, H.J., 2005. Glacier and lake-level variations in west-central Europe over the last 3500 years. The Holocene 15, 789–801. https://doi.org/10.1191/0959683605hl853ra.
IPCC, 2019. IPCC Special Report on Climate Change and Land. An IPCC Special Report on Climate Change, Desertification, Land Degradation, Sustainable Land Management, Food Security, and Greenhouse Gas Fluxes in Terrestrial Ecosystems.
Kaplan, J.O., Krumhardt, K.M., Ellis, E.C., Ruddiman, W.F., Lemmen, C., Goldewijk, K.K., 2011. Holocene carbon emissions as a result of anthropogenic land cover change. The Holocene 21, 775–791. https://doi.org/10.1177/0959683610386983.
Krishnaswamy, S., Lal, D., Martin, J.M., Meybeck, M., 1971. Geochronology of lake sediments. Earth Planet. Sci. Lett. 11, 407–414. https://doi.org/10.1016/0012-821X(71)90202-0.
Lal, R., 2003. Soil erosion and the global carbon budget. Environ. Int. 29, 437–450. https://doi.org/10.1016/S0160-4120(02)00192-7.
Le Roy, M., Nicolussi, K., Deline, P., Astrade, L., Edouard, J.-L., Miramont, C., Arnaud, F., 2015. Calendar-dated glacier variations in the western European Alps during the Neoglacial: the Mer de Glace record, Mont Blanc massif. Quat. Sci. Rev. 108, 1–22. https://doi.org/10.1016/j.quascirev.2014.10.033.
Magny, M., Bossuet, G., Ruffaldi, P., Leroux, A., Mouthon, J., 2011. Orbital imprint on Holocene palaeohydrological variations in west-central Europe as reflected by lake-level changes at Cerin (Jura Mountains, eastern France). J. Quat. Sci. 26, 171–177. https://doi.org/10.1002/jqs.1436.
Martini, J., 1966. Etude pétrographique des grés de Taveyanne entre Arve et Giffre (Haute Savoie, France). Université de Genève, Alpes (Theses).
MEA, M.E.A, 2005. Ecosystems and Human Well-Being: Wetlands and Water. World Resources Institute, Washington, DC, pp. 5.
Moreno, A., Valero-Garcés, B.L., González-Sampériz, P., Rico, M., 2008. Flood response to rainfall variability during the last 2000 years inferred from the Taravilla Lake record (Central Iberian Range, Spain). J. Paleolimnol. 40, 943–961. https://doi.org/10.1007/s10933-008-9209-3.
Mougin, P., 1914. Les torrents de la Savoie. La Fontaine de Siloé.
Mourier, B., Poulenard, J., Chauvel, C., Faivre, P., Carcaillet, C., 2008. Distinguishing subalpine soil types using extractible Al and Fe fractions and REE geochemistry. Geoderma 145, 107–120. https://doi.org/10.1016/j.geoderma.2008.03.001.
Nicolussi, K., Kaufmann, M., Patzelt, G., Plicht van der, J., Thurner, A., 2005. Holocene tree-line variability in the Kauner Valley, Central Eastern Alps, indicated by dendrochronological analysis of living trees and subfossil logs. Veg. Hist. Archaeobotany 14, 221–234. https://doi.org/10.1007/s00334-005-0013-y.
Noren, A.J., Bierman, P.R., Steig, E.J., Lini, A., Southon, J., 2002. Millennial-scale storminess variability in the northeastern United States during the Holocene epoch. Nature 419, 821.
Parducci, L., Bennett, K.D., Ficetola, G.F., Alsos, I.G., Suyama, Y., Wood, J.R., Pedersen, M.W., 2017. Ancient plant DNA in lake sediments. New Phytol. 214, 924–942.

https://doi.org/10.1111/nph.14470.
R Development Core Team, 2011. R: A Language and Environment for Statistical Computing. R Foundation for Statistical Computing, Vienna, Austria.
Rapuc, W., Sabatier, P., Arnaud, F., Palumbo, A., Develle, A.-L., Reyss, J.-L., Augustin, L., Régnier, E., Piccin, A., Chapron, E., Dumoulin, J.-P., von Grafenstein, U., 2019. Holocene-long record of flood frequency in the Southern Alps (Lake Iseo, Italy) under human and climate forcing. Glob. Planet. Chang. 175, 160–172. https://doi.org/10.1016/j.gloplacha.2019.02.010.
Reimer, P.J., Bard, E., Bayliss, A., Beck, J.W., Blackwell, P.G., Bronk Ramsey, C., Buck, C. E., Cheng, H., Edwards, R.L., Friedrich, M., 2013. IntCal13 and Marine13 radiocarbon age calibration curves 0–50,000 years cal BP.
Rey, P.-J., 2008. Premières occupations de la montagne sur les versants du col d'Anterne (2 257 m). ADLFI. Archéologie de la France-Informations. une revue Gallia.
Rey, P.-J., 2010. Passy-Servoz. Les premières occupations humaines des versants du col d'Anterne. Bilan scientifique de la Région Rhône-Alpes. pp. 198–200.
Rey, P.-J., Batigne-Vallet, C., Collombet, J., Delhon, C., Martin, L., Moulin, B., Poulenard, J., Scoccimaro, N., Sordoillet, D., Thiebault, S., et al., 2008. Approche archéologique et environnementale des premiers peuplements alpins autour du col du Petit Saint-Bernard (Savoie, Vallée d'Aoste): un bilan d'étape. In: Archéologie de l'espace Montagnard: Confrontation d'expériences Européennes, pp. 197–210.
Reyss, J.-L., Schmidt, S., Legeleux, F., Bonté, P., 1995. Large, low background well-type detectors for measurements of environmental radioactivity. Nucl. Inst. Methods Phys. Res. A 357, 391–397.
Robbins, J.A., Edgington, D.N., 1975. Determination of recent sedimentation rates in Lake Michigan using Pb-210 and Cs-137. Geochim. Cosmochim. Acta 39, 285–304.
Sabatier, P., Bruno, W., Francesco, F.G., Fanny, M., Jérôme, P., Anne-Lise, D., Adeline, B., Wentao, C., Cécile, P., Jean-Louis, R., Ludovic, G., Manon, B., Yves, P., Emmanuel, M., Pierre, T., Fabien, A., 2017. 6-kyr record of flood frequency and intensity in the western Mediterranean Alps – interplay of solar and temperature forcing. Quat. Sci. Rev. 170, 121–135. https://doi.org/10.1016/j.quascirev.2017.06.019.
Sesiano, J., 1993. Monographie physique des plans d'eau naturels du département de la Haute-Savoie, France.
Shand, C.A., Wendler, R., 2014. Portable X-ray fluorescence analysis of mineral and organic soils and the influence of organic matter. J. Geochem. Explor. 143, 31–42. https://doi.org/10.1016/j.gexplo.2014.03.005.
Stacy, E.M., Hart, S.C., Hunsaker, C.T., Johnson, D.W., Berhe, A.A., 2015. Soil carbon and nitrogen erosion in forested catchments: implications for erosion-induced terrestrial carbon sequestration. Biogeosciences 12, 4861–4874. https://doi.org/10.5194/bg-12-4861-2015.
Sturm, M., Matter, A., 1978. Turbidites and Varves in Lake Brienz (Switzerland): Deposition of Clastic Detritus by Density Currents. Wiley Online Library.
Talon, B., 2006. Analyses anthracologiques au col du Petit St-Bernard. Archéoanthracologie et pédoanthracologie. In: Actes Du Séminaire de Clôture Du Programme INTERREG III A ALCOTRA 2000–2006: Alpis Graia. Archéologie sans Frontière Au Col Du Petit St-Bernard. Aoste, pp. 51–58.
Vanmaercke, M., Poesen, J., Govers, G., Verstraeten, G., 2015. Quantifying human impacts on catchment sediment yield: a continental approach. Glob. Planet. Chang. 130, 22–36. https://doi.org/10.1016/j.gloplacha.2015.04.001.
Verheijen, F.G.A., Jones, R.J.A., Rickson, R.J., Smith, C.J., 2009. Tolerable versus actual soil erosion rates in Europe. Earth Sci. Rev. 94, 23–38. https://doi.org/10.1016/j.earscirev.2009.02.003.
Wang, Z., Hoffmann, T., Six, J., Kaplan, J.O., Govers, G., Doetterl, S., Van Oost, K., 2017. Human-induced erosion has offset one-third of carbon emissions from land cover change. Nat. Clim. Chang. 7, 345–349. https://doi.org/10.1038/nclimate3263.
Wick, L., van Leeuwen, J.F., van der Knaap, W.O., Lotter, A.F., 2003. Holocene vegetation development in the catchment of Sägistalsee (1935 m asl), a small lake in the Swiss Alps. J. Paleolimnol. 30, 261–272.
Wilhelm, B., Arnaud, F., Sabatier, P., Crouzet, C., Brisset, E., Chaumillon, E., Disnar, J.-R., Guiter, F., Malet, E., Reyss, J.-L., Tachikawa, K., Bard, E., Delannoy, J.-J., 2012. 1400 years of extreme precipitation patterns over the Mediterranean French Alps and possible forcing mechanisms. Quat. Res. 78, 1–12. https://doi.org/10.1016/j.yqres.2012.03.003.
Wilhelm, B., Ballesteros Canovas, J.A., Corella Aznar, J.P., Kämpf, L., Swierczynski, T., Stoffel, M., Støren, E., Toonen, W., 2018. Recent advances in paleoflood hydrology: from new archives to data compilation and analysis. Water Secur. 3, 1–8. https://doi.org/10.1016/j.wasec.2018.07.001.
Wilhelm, B., Ballesteros Cánovas, J.A., Macdonald, N., Toonen, W.H.J., Baker, V., Barriendos, M., Benito, G., Brauer, A., Corella, J.P., Denniston, R., Glaser, R., Ionita, M., Kahle, M., Liu, T., Luetscher, M., Macklin, M., Mudelsee, M., Munoz, S., Schulte, L., St. George, S., Stoffel, M., Wetter, O., 2019. Interpreting historical, botanical, and geological evidence to aid preparations for future floods. Wiley Interdiscip. Rev. Water 6, e1318. https://doi.org/10.1002/wat2.1318.
Wirth, S.B., Glur, L., Gilli, A., Anselmetti, F.S., 2013. Holocene flood frequency across the Central Alps – solar forcing and evidence for variations in North Atlantic atmospheric circulation. Quat. Sci. Rev. 80, 112–128. https://doi.org/10.1016/j.quascirev.2013.09.002.
WRB - FAO, 2014. World Reference Base for Soil Resources 2014 International Soil Classification System for Naming Soils and Creating Legends for Soil Maps. FAO, Rome.